

Synchronization and phase locking in two-dimensional arrays of Josephson junctions

C. B. Whan,* A. B. Cawthorne, and C. J. Lobb

Center for Superconductivity Research, Department of Physics, University of Maryland, College Park, Maryland 20742

(Received 3 October 1995)

We report numerical studies of phase locking in two-dimensional (2D) arrays of Josephson junctions. In the conventional 2D arrays biased with dc current in the horizontal (X) direction, the phase-locked solution is only possible in arrays with no disorder. In the presence of disorder in the junction critical currents, we see vertical (Y) columns of phase locked clusters form in the array with no intercolumn locking. As an extension, we introduced a geometry called XY -biased array, where the array is biased in both X and Y directions. In XY -biased array we found a dynamical state, where all junction voltages are strictly dc and the only oscillating components are the supercurrents in each junction. This dynamical state is stable against experimentally achievable disorder in the junction critical currents.

I. INTRODUCTION

Studies of synchronization phenomena in coupled nonlinear oscillators have broad scientific and technological interest.¹⁻⁷ Josephson-junction arrays, when biased in the voltage state, are well-characterized coupled oscillator systems with important potential for high-frequency applications. One of the major challenges in building practical Josephson-junction array oscillators is getting all the junctions in the array to synchronize, in order to get coherent high power output.⁸⁻¹⁴

In this paper, we use numerical simulations to investigate phase locking in two-dimensional (2D) arrays of Josephson junctions. In our analysis, we do not include a load circuit. This enables us to study the intrinsic phase-locking capability of the array due to internal coupling of the junctions.

Our initial interest in this problem was inspired by the work of Aoyagi and Kuramoto.⁵ These authors studied a general nearest-neighbor-coupled oscillator lattice with randomly distributed frequencies. Their numerical results indicated a frequency locking transition in two-dimensional lattices as the coupling strength between nearest-neighbor oscillators is increased.

Previously, Hadley and co-workers¹⁰ have analyzed the linear stability of the in-phase (synchronized) solution in Josephson-junction series (1D) arrays and found that the in-phase solution is neutrally stable (meaning that a perturbation would neither grow nor shrink within a linear approximation) for small perturbations. They generalized their result to 2D arrays by noting that the vertical (Y) junctions in an array biased in the horizontal (X) direction are inactive and the active X junctions across a column share a common voltage. This led them to conclude that in an unloaded 2D array the in-phase solution is also neutrally stable.

More recently, the analytic calculations of Wiesenfeld *et al.*¹³ and the numerical simulations of Kautz¹⁴ showed similar behavior. In Kautz's simulation, he explicitly removed the inactive Y junctions and connected the neighboring islands with pure inductors. This approach still leaves open the question of the role played by the Y junctions, or, for that matter, if they play any role at all. The Y junctions are considered inactive in the sense that they normally do not

have a net dc voltage across them and therefore do not have sustained Josephson oscillations. Small amplitude plasma oscillations,¹⁵ however, can affect the coupling among the active X junctions, especially in the underdamped regime. Indeed, Geigenmüller *et al.*¹⁶ showed that the small amplitude "spin fluctuations" in 2D underdamped arrays play a profound role in the vortex dynamics of this system.

The method we use in this paper is largely based on the method used by Sakaguchi *et al.*³ Here we will briefly outline it.

Consider a pair of nearest-neighbor junctions n and m . The phase differences in the superconducting order parameter across each junction are γ_n and γ_m , respectively. We consider the two junctions synchronized if the difference between the phase differences, $\Delta\gamma_{nm} = \gamma_n - \gamma_m$, stays constant with respect to time. This would guarantee that the two junctions have identical voltages, i.e.,

$$v_n - v_m = \frac{d(\Delta\gamma_{nm})}{d\tau} = 0.$$

In practice, we require,

$$|\Delta\gamma_{nm}(\tau_0 + \tau) - \Delta\gamma_{nm}(\tau_0)| < \epsilon, \quad (1)$$

for a small ϵ and a long time τ . In our simulations, we choose $\epsilon = 10^\circ$ and vary τ .

Imagine we apply the criterion, Eq. (1), to all nearest-neighbor-pair junctions in the array. Each time we find a pair that is synchronized [according to Eq. (1)], we put an imaginary bond connecting the two junctions in that pair.¹⁷ After we are finished, we might expect to see one or more synchronized clusters in the array. Within each cluster all junctions are synchronized to one another and are interconnected by the imaginary bonds. Figure 1 illustrates a possible scenario.

We now follow Sakaguchi *et al.*³ and define a synchronization order parameter

$$r = \lim_{N \rightarrow \infty} \frac{N_s}{N}, \quad (2)$$

where N_s is the number of junctions in the largest synchronized clusters and N is the total number of junctions on the

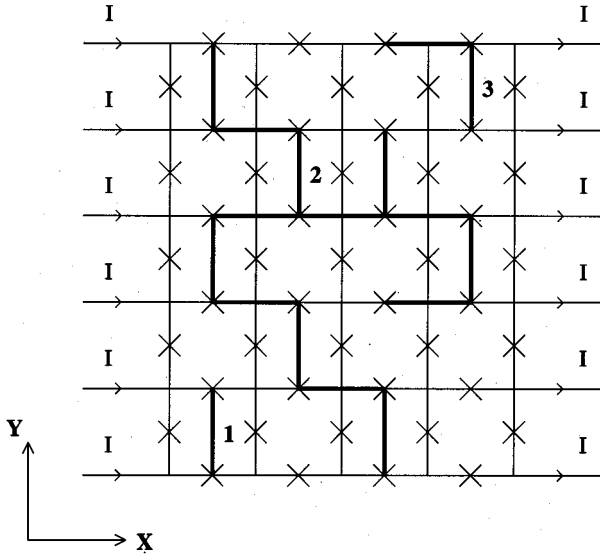


FIG. 1. A sketch illustrating synchronized clusters and the definition of the order parameter r . Each pair of nearest-neighbor junctions are connected by a bond (heavy lines) if they synchronize to one another according to the criterion in the text. In this figure, there are three synchronized clusters. The largest cluster is cluster 2 and it contains 15 junctions. Therefore the order parameter $r = 15/24$. Note here we count the X junctions only, since the Y junctions have no sustained oscillations.

lattice. In the case of complete synchronization, $r = 1$. Otherwise, in general, $r < 1$. In principle, r should be averaged over a statistical ensemble, but in practice we often average it on 3–5 samples, which nevertheless appears to give reasonable results. In order to compute the order parameter r , the synchronized clusters need to be labeled. We use an efficient algorithm due to Hoshen and Kopelman¹⁸ to automate the cluster labeling procedure.

In the next section, we discuss a conventional 2D array design, which is current biased in the X direction, and study the synchronization with and without disorder in the critical currents. In Sec. III, we introduce an array design, where the array is current biased in both X and Y directions, and discuss the dynamical states that are made available by this simple extension. Section IV is a brief summary and conclusions.

II. X-BIASED ARRAY

In Fig. 2, we show a sketch of a conventional 2D array biased in the X direction, with equal amount of current I injected into each node of the column on the left-hand side and extracted from the corresponding nodes on the right-hand side. Each junction is described by the usual resistively-capacitively shunted junction (RCSJ) model.¹⁵ For example, for the junction connecting islands n and m , we have

$$i_{nm} = \beta_C \ddot{\gamma}_{nm} + \dot{\gamma}_{nm} + \alpha_{nm} \sin(\gamma_{nm}), \quad (3)$$

$$v_{nm} = \dot{\gamma}_{nm},$$

and on each node current conservation is enforced, i.e.,

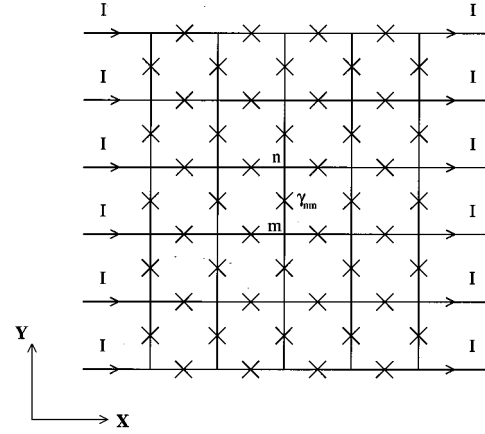


FIG. 2. A sketch of a 5×6 2D array biased in the X direction. Each cross represents a Josephson junction.

$$\sum_{m \in \text{NN}} i_{nm} = i_n^{\text{ext}}. \quad (4)$$

Here i_n^{ext} denotes the external current injected at each node. For our X -biased array,

$$i_n^{\text{ext}} = \begin{cases} i & \text{if } n \in \text{left boundary} \\ -i & \text{if } n \in \text{right boundary.} \end{cases} \quad (5)$$

The normalization convention we have adopted here is fairly standard. The currents are normalized to the *average* single-junction critical current \bar{I}_c and voltages are normalized to $\bar{I}_c R$. Here R is the single-junction resistance which is assumed to be the same for all junctions. We also assume all junction capacitances are the same.

The only disorder we consider here is the spread in the junction critical currents, which we expect to be the dominating factor in most experimental situations due to their exponential dependences on the barrier thickness in tunnel junctions. We characterize this disorder using Gaussian-distributed random numbers,¹⁹

$$\alpha_{nm} = \frac{I_c^{nm}}{\bar{I}_c} \quad (6)$$

with mean $\bar{\alpha}_{nm} = 1$, and standard deviation σ .

In Eq. (3), γ_{nm} is the phase difference of the superconducting order parameter across the junction connecting islands n and m , and the overdots denote time derivatives with respect to the normalized time $\tau = \omega_c t = 2\pi \bar{I}_c R t / \Phi_0$. β_C is the average Stewart-McCumber parameter of the single junctions,

$$\beta_C = \frac{2\pi \bar{I}_c R^2 C}{\Phi_0}. \quad (7)$$

We solve the complete array dynamical equations, Eqs. (3)–(5), using a simple Euler method assisted by an efficient fast-Fourier-transform capacitance matrix inversion scheme.^{16,20} During the integration process, we can compute and monitor the order parameter $r(\tau)$, defined in the previous section. When applying the synchronization criterion,

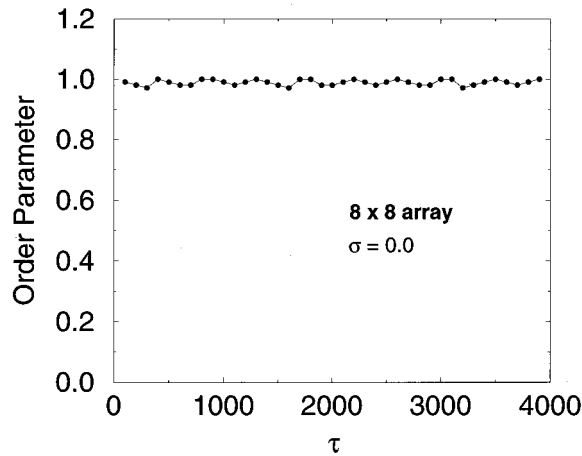


FIG. 3. Synchronization order parameter r plotted against time for an 8×8 array made of identical junctions ($\sigma=0.0$). The parameter values are $\beta_C=9.0$ and $i=1.20$. Notice $r \approx 1.0$ throughout the observation period, indicating that a complete synchronization is possible for a uniform array.

Eq. (1), we will only consider the X junctions, since the Y junctions, in general, will have no sustained ac Josephson oscillations.

In Fig. 3, we show an r vs τ plot for an array of size 8×8 with no critical current disorder, i.e., $\sigma=0.0$. The parameter values are $\beta_C=9.0$ and $i=1.2$. We see from Fig. 3 that in a uniform array of identical junctions, the order parameter always stays close to $r=1$, indicating that none of the junction phases grow relative to their nearest neighbors. Therefore, a synchronized solution can and does exist in the system as long as the junctions are identical.

The synchronized solution becomes unstable when we introduce some disorder in the junction critical currents. Figure 4 is a plot similar to Fig. 3, but for a disordered array with $\sigma=0.10$. The array size is 16×16 , and $\beta_C=9.0$, $i=1.20$. There is obviously no synchronization in this disordered array, since the order parameter rapidly decays and reaches a

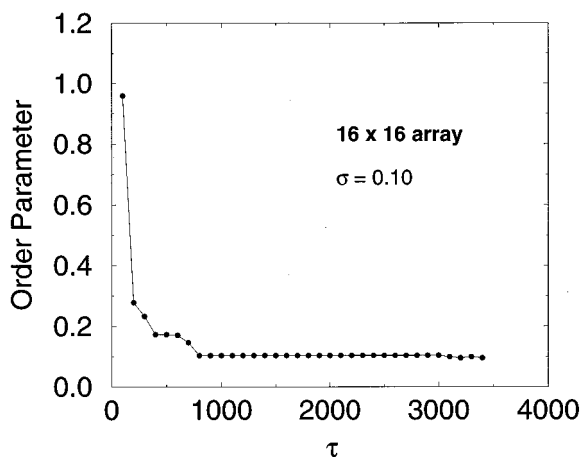


FIG. 4. Synchronization order parameter r plotted against time for a 16×16 array with disordered junction critical currents, $\sigma=0.10$. The other parameter values are $\beta_C=9.0$ and $i=1.20$. Notice r decays rapidly towards a value much smaller than one, indicating lack of synchronization in this disordered array.

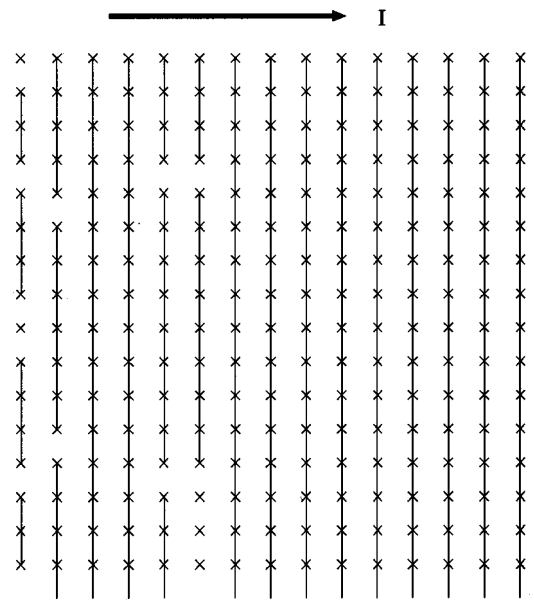


FIG. 5. Synchronized clusters in a disordered X -biased 16×16 array. Here $\sigma=0.10$, $\beta_C=9.0$, and $i=1.20$. The snapshot is taken at $\tau=3500$.

value much less than unity. We did a similar calculation for $\sigma=0.01$. The result is essentially the same, except the decay of r is less rapid, which seems to indicate that the synchronized solution is always unstable in the presence of finite amount of disorder.

In the disordered array, it is instructive to look at the picture of the actual synchronized clusters after the order parameter has settled to a final value. Figure 5 is a snapshot, taken at $\tau=3500$, of the clusters in the array that corresponds to Fig. 4. If the entire array is synchronized, we should see a single cluster spanning the whole array. Instead, what we see in Fig. 5 are vertical lines connecting junctions along the Y columns, indicating that the junctions along the Y direction are mostly synchronized, despite the spread in the critical currents. We do not see any horizontal lines connecting the vertical column clusters, which means that the columns are decoupled from one another and no longer synchronize. Thus we conclude that in this nonuniform 2D array biased in the X direction, the final solution of the system is made up of synchronized columns along the Y direction. The intercolumn locking is broken by disorder. Although other authors have previously reached similar conclusions^{10,13,14} our cluster analysis explicitly demonstrates how synchronization is destroyed by disorder.

III. XY-BIASED ARRAY

As we saw in the previous section, in X -biased arrays the intercolumn locking is broken by disorder even though within a Y column the junctions do tend to synchronize. This is not very useful in practice, since real arrays always have some disorder (with current technology, $\sigma=0.01$ perhaps is the limit), and without intercolumn locking each column can oscillate completely independently and the entire array will be incoherent.

Although complete synchronization in a disordered

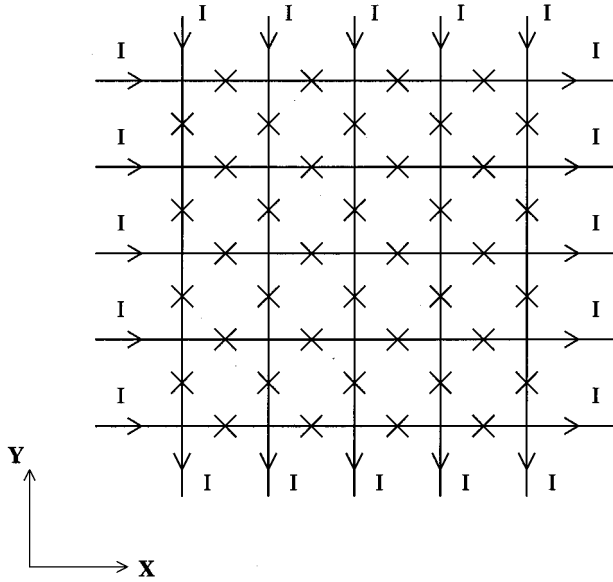


FIG. 6. Sketch of an XY -biased array. An equal amount of current is injected into every node at the left and top boundaries and extracted from the remaining two (i.e., right and bottom) boundaries.

X -biased array is difficult to achieve, the fact that the Y junctions in the same column prefer to be locked gives us some hint on how the design might be improved. Since X bias induces synchronization along Y columns, by symmetry we would expect that Y bias should induce synchronization along X rows. Then the next natural question is what happens if we bias the array along both X and Y directions, as shown in Fig. 6. This design, which we call XY -biased array, has the advantage that every junction in the array is biased in the voltage state and therefore oscillating. Thus we can treat both the X junctions and the Y junctions on an equal footing. This also brings us closer to the model originally studied by Kuramoto and co-workers.^{3,5}

To proceed, we define a quantity to measure phase coherence, the variance of all nearest-neighbor junction phase differences,

$$\langle \Delta \gamma(\tau) \rangle = A \sum_{\langle n,m \rangle} [\gamma_n(\tau) - \gamma_m(\tau)]^2. \quad (8)$$

Here the summation is over all nearest-neighbor pairs of junctions and A is a constant chosen to normalize $\langle \Delta \gamma \rangle$ to a convenient value. Note we are considering *all* junctions here, instead of only the X junctions as we did for X -biased arrays in the previous section.

In Fig. 7, we show $\langle \Delta \gamma(\tau) \rangle$ vs τ plot for a 4×4 array with and without disorder. The parameter values are $\beta_C = 9.0$ and $i = 2.0$. The solid curve in Fig. 7 corresponds to a uniform 4×4 array, while the dashed curve corresponds to a disordered array (with $\sigma = 0.10$) of the same size. From Fig. 7, we see that the system reaches a phase-locked state after some transient oscillations, since $\langle \Delta \gamma(\tau) \rangle$ saturates to a constant value and stays there. Moreover, this phase-locked state is reached in the presence of a fairly large disorder, $\sigma = 0.10$ (notice the dashed curve in Fig. 7 also saturates).

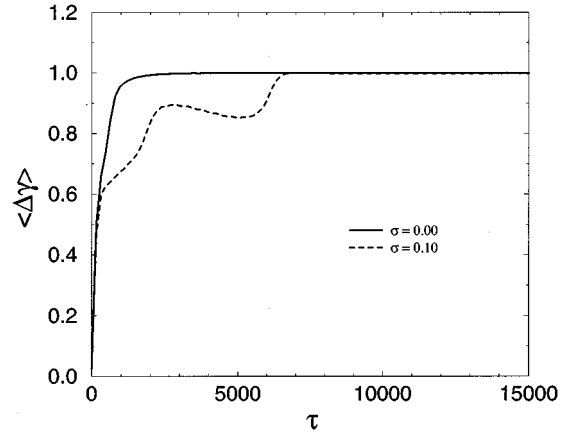


FIG. 7. The phase variance $\langle \Delta \gamma \rangle$ of nearest-neighbor junctions is plotted as a function of time for a 4×4 array. The parameter values are $\beta_C = 10$ and $i = 2.0$. From the figure, we see that XY -biased array approaches a phase-locked state after some transient, and moreover, this state is stable even in the presence of disorder. Here we chose the normalization such that the saturated values of $\langle \Delta \gamma \rangle$ is one.

This latter point is of great importance, since any dynamical state of the system has to be stable against disorder in order to be experimentally relevant.

To get a better understanding of the nature of this phase locked dynamical state, we consider the simplest nontrivial case—a 2×2 XY -biased array. Figure 8 shows the variance of the phase differences $\langle \Delta \gamma \rangle$, along with all four junction voltages, as functions of time. The parameter values in Fig. 8 are the same as in Fig. 7. As we can see, the junction voltages oscillate in the transient state, but in the locked state *all* junctions have the same constant dc value $v = 2$. In general the constant voltage is given by $v = i$ in our normalized units. This means once the system reaches the locked state, there is no oscillating voltage anywhere in the system. There is, however, oscillating supercurrent $\sin(\gamma_n)$. Since the voltage $v = i$ is a constant, we have

$$\gamma_n = i\tau + \psi_n, \quad (9)$$

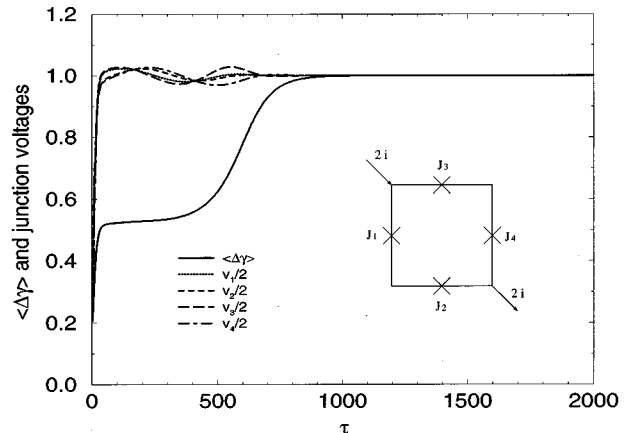


FIG. 8. Time dependences of $\langle \Delta \gamma \rangle$ and all the junction voltages in a 2×2 XY -biased array. The array geometry is shown in the inset. Notice that once the system reaches the synchronized state, the voltages on all the junctions cease to oscillate and there are only dc voltages.

where ψ_n is an arbitrary constant. The corresponding supercurrent

$$\sin(\gamma_n) = \sin(i\tau + \psi_n), \quad (10)$$

is a pure sine wave with the frequency determined by the dc bias current i .

In the simple case of a 2×2 uniform ($\sigma=0$) array, we can demonstrate analytically how such a special type of solution occurs. A 2×2 XY -biased array consists of four junctions and four nodes, as sketched in the inset of Fig. 8. Note at the nodes on the upper left corner and lower right corner, the bias currents along X and Y directions add and give $2i$ and $-2i$ respectively. At the other two nodes (upper right and lower left corners), the bias currents cancel. The dynamical equations for this system are

$$i_1 = \beta_C \dot{\gamma}_1 + \dot{\gamma}_1 + \sin(\gamma_1), \quad (11)$$

$$i_1 = \beta_C \dot{\gamma}_2 + \dot{\gamma}_2 + \sin(\gamma_2), \quad (12)$$

$$i_2 = \beta_C \dot{\gamma}_3 + \dot{\gamma}_3 + \sin(\gamma_3), \quad (13)$$

$$i_2 = \beta_C \dot{\gamma}_4 + \dot{\gamma}_4 + \sin(\gamma_4), \quad (14)$$

$$i_1 + i_2 = 2i, \quad (15)$$

$$\dot{\gamma}_1 + \dot{\gamma}_2 = \dot{\gamma}_3 + \dot{\gamma}_4. \quad (16)$$

We first eliminate i_1 and i_2 in the above set of equations and solve for the γ 's. The locked constant voltage solution

$$\dot{\gamma}_1 = \dot{\gamma}_2 = \dot{\gamma}_3 = \dot{\gamma}_4 = i, \quad (17)$$

can exist if the following conditions are satisfied:

$$\sin(\gamma_1) + \sin(\gamma_3) = \sin(\gamma_2) + \sin(\gamma_4) = 0, \quad (18)$$

$$\sin(\gamma_1) - \sin(\gamma_2) = \sin(\gamma_3) - \sin(\gamma_4) = 0. \quad (19)$$

The final solution, in terms of γ 's, is

$$\gamma_1 = \gamma_2 = i\tau + \psi_0, \quad (20)$$

$$\gamma_3 = \gamma_4 = i\tau + \pi + \psi_0, \quad (21)$$

where ψ_0 is an arbitrary constant. One can easily check that this solution guarantees that all junctions have constant voltage $v=i$. The oscillating supercurrents give rise to a sinusoidal circulating current

$$i_{\text{circ}} \equiv i_1 - i_2 = 2\sin(i\tau + \psi_0) \quad (22)$$

in the loop. Figure 9 illustrates this special solution.

If we convert Eq. (22) back to our original units, we have,

$$I_{\text{circ}} \equiv I_C i_{\text{circ}} = 2I_c \sin(\omega_I t + \psi_0), \quad (23)$$

with

$$\omega_I = i\omega_c = \frac{2eIR}{\hbar}. \quad (24)$$

Therefore a 2×2 XY -biased array is a purely sinusoidal current dipole oscillator with the frequency conveniently tuned by the dc bias current. However, it suffers from the same

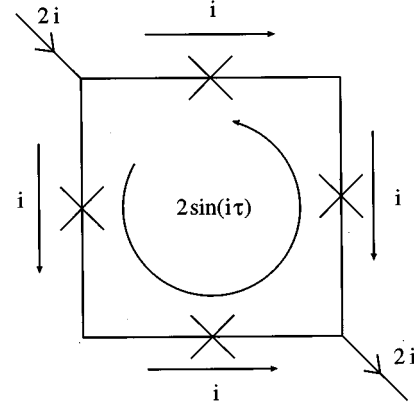


FIG. 9. Illustration of the special phase locked state in a 2×2 XY -biased array. All junction voltages are $v=i$ and there is a circulating supercurrent $2\sin(i\tau + \psi_0)$ in the loop.

drawback as other Josephson oscillators with few junctions. The maximum power available for radiation (to free space) is on the order of 1 nW.

For arrays larger than 2×2 , the phase locked solution is much more complicated. First of all we cannot have every plaquette maintaining a circulating sinusoidal supercurrent and keep all of them in phase from plaquette to plaquette. If this were to happen, we are left with a situation where all internal oscillating currents cancel and the only supercurrent oscillations are confined to the boundaries. However, we saw in Fig. 8 that every junction carries a constant dc voltage, therefore all the supercurrents have to oscillate according to Josephson's second equation, Eq. (3).

Another complication arises due to the symmetry in the uniform array. In a large uniform array, there are many different relative phase configurations that an array can lock to, even for a single bias current value. One might expect something similar to the attractor crowding phenomena observed in series arrays²¹ may also occur in this case. The exact phase configurations in larger arrays are unclear at present and need further investigation. Our preliminary results suggest that the system tends to 'hop' or even drift very slowly between equivalent phase configurations, while still maintaining constant voltages on each individual junctions.

So far in this paper, we have ignored inductive effects altogether. In real samples there will inevitably be some inductance, which includes the cell inductance, mutual inductance among different cells, and junction parasitics. The cell inductances and the mutual inductances can be reduced by putting down a superconducting ground plane underneath the sample. The parasitics, on the other hand, are more difficult to eliminate.²² Darula *et al.*²³ have studied linear Josephson-junction arrays closed into a superconducting loop. They were able to find a stable phase-locked state in their system in a wide range of inductance parameters. Their system, when simplified to the smallest nontrivial unit with four junctions, is equivalent to our smallest (2×2) XY -biased array with the cell inductance included. Therefore we know that at least in the 2×2 XY -biased array, our special synchronized state survives when cell inductances are included. For larger arrays, analysis including inductance is not available at the moment.

Experimentally, Beuven *et al.*²⁴ studied 2×2 high- T_c junction arrays with large inductances. Using additional current compensation, they found a range of total bias current where all junctions have the same dc voltage. Larger XY -biased arrays have yet to be implemented. One might wonder whether the XY -biased array is simply equivalent to the diagonally biased square array, such as those studied by Sohn *et al.*²⁵ While an infinite size XY -biased array should be equivalent to diagonally biased array, they are different at finite size due to extra constraints applied by the boundary conditions at all *four* edges of the XY -biased array (see Fig. 6). It is not clear, however, whether such a distinction is crucial for the existence of the locked state.

IV. CONCLUSION

We have studied phase locking in two-dimensional arrays of Josephson junctions by numerically solving the full 2D array dynamical equations. In a conventional 2D square array biased along the X direction, we found that a completely synchronized solution is possible only for a uniform array. When a small amount of disorder is included in the junction critical currents, the synchronized array is broken into synchronized column clusters along Y direction with no inter-column locking along X direction.

To improve the coupling among junctions, we propose an array design in which one biases the 2D square array along both X and Y directions. In this XY -biased array, we found a synchronized dynamical state, where all junction voltages stay purely dc while all currents oscillate. More importantly, the dynamical state is stable in arrays with disorders up to $\sigma=0.10$. This level of uniformity can be easily achieved with current fabrication technology. For a small 2×2 XY -biased array, we obtained an analytical expression for the dynamical state, which consists of a sinusoidal circulating loop current acting like a dipole current oscillator with the frequency directly tuned by the dc bias current. The detailed nature of the dynamical state in larger arrays is currently unclear and needs further investigation. Other interesting directions for future investigations include taking into account all the inductances in the circuit, as well as the effects of magnetic field and thermal noise.

ACKNOWLEDGMENTS

We thank Fred Wellstood and Ulrich Geigenmüller for a critical reading of the manuscript. This work was supported by the U.S. Air Force Office of Scientific Research under Grant No. F49620-92-J-0041, and the State of Maryland through the Center for Superconductivity Research.

*Current address: Department of Electrical Engineering and Computer Science, Massachusetts Institute of Technology, 77 Massachusetts Avenue, Cambridge, Massachusetts 02139.

¹A. T. Winfree, *The Geometry of Biological Time* (Springer, New York, 1980).

²Y. Kuramoto, *Chemical Oscillations, Waves, and Turbulence* (Springer, Berlin, 1984).

³H. Sakaguchi, S. Shinomoto, and Y. Kuramoto, *Prog. Theor. Phys.* **76**, 576 (1986).

⁴S. H. Strogatz and R. E. Mirollo, *Physica D* **31**, 143 (1988).

⁵T. Aoyagi and Y. Kuramoto, *Phys. Lett. A* **155**, 410 (1991).

⁶M. Bahiana and M. S. O. Massunaga, *Phys. Rev. E* **49**, 3558 (1994).

⁷G. Grinstein, D. Mukamel, R. Seidin, and C. H. Bennett, *Phys. Rev. Lett.* **70**, 3607 (1993).

⁸A. K. Jain, K. K. Likharev, J. E. Lukens, and J. E. Sauvageau, *Phys. Rep.* **109**, 309 (1984).

⁹J. E. Lukens, A. K. Jain, and K. L. Wan, in *Superconducting Electronics*, edited by H. Weinstock and M. Nisenoff (Springer-Verlag, New York, 1989).

¹⁰P. Hadley, M. R. Beasley, and K. Wiesenfeld, *Appl. Phys. Lett.* **52**, 1619 (1988); *Phys. Rev. B* **38**, 8712 (1988); P. Hadley, Ph.D. thesis, Stanford University, 1989.

¹¹S. P. Benz and C. J. Burroughs, *Appl. Phys. Lett.* **58**, 2162 (1991).

¹²M. Octavio, C. B. Whan, and C. J. Lobb, *Appl. Phys. Lett.* **60**, 766 (1992).

¹³K. Wiesenfeld, S. P. Benz, and P. A. A. Booij, *J. Appl. Phys.* **76**, 3835 (1994).

¹⁴R. L. Kautz, *IEEE Trans. Appl. Supercond.* **5**, 2702 (1995).

¹⁵K. K. Likharev, *Dynamics of Josephson Junctions and Circuits* (Gordon and Breach, New York, 1986).

¹⁶U. Geigenmüller, C. J. Lobb, and C. B. Whan, *Phys. Rev. B* **47**, 348 (1993).

¹⁷The bond here only serves as a graphical indicator that the two junctions are synchronized. It should not be confused with physical wire connections.

¹⁸J. Hoshen and R. Kopelman, *Phys. Rev. B* **14**, 3438 (1976).

¹⁹We actually use a truncated Gaussian distribution,

$$P(\alpha) = \begin{cases} \frac{1}{\sqrt{2\pi\sigma}} \exp\left[-\frac{(\alpha-1)^2}{2\sigma^2}\right] & \text{if } \alpha \geq 0 \\ 0 & \text{if } \alpha < 0, \end{cases}$$

to avoid unphysical negative critical currents. This distribution, rigorously speaking, is incorrect since it is not properly normalized due to the truncation. The error, however, is small for small values of σ ($\sigma < 0.10$) that we consider here.

²⁰H. Eikmans and J. E. van Himbergen, *Phys. Rev. B* **41**, 8927 (1990).

²¹Kurt Wiesenfeld and Peter Hadley, *Phys. Rev. Lett.* **62**, 1335 (1989).

²²A. B. Cawthorne, C. B. Whan, and C. J. Lobb (unpublished).

²³M. Darula, S. Beuven, M. Siegel, A. Darulova, and P. Seidel, *Appl. Phys. Lett.* **67** 1618 (1995).

²⁴S. Beuven, M. Darula, J. Schubert, W. Zander, M. Siegel, and P. Seidel, *IEEE Trans. Appl. Supercond.* **5**, 3288 (1995).

²⁵L. L. Sohn, M. S. Rzchowski, J. U. Free, S. P. Benz, M. Tinkham, and C. J. Lobb, *Phys. Rev. B* **44**, 925 (1991).